Earthquake-triggered displacements in the central Salton Trough reveal wide range of slip modes

Kathryn Materna[1], M. Morow Tan[1]
1. CIRES and Department of Geological Sciences, University of Colorado Boulder

University of Colorado Boulder
CIRES

Introduction and Project Objectives

Centimeter-scale triggered creep was widely documented on Southern California faults following the April 3 2010 El Mayor-Cucapah (EMC) M7.2 earthquake (Wei et al., 2011; Donnellan et al., 2014; Rymer et al., 2010). Aseismic creep was observed on the Superstition Hills, San Andreas, Elmore Ranch, Imperial, and Brawley faults, as well as many other smaller faults. Most of the triggered creep was right-lateral strike slip, with smaller amounts of left-lateral strike slip on the Elmore Ranch fault and normal faulting on the Brawley fault.

In this project, we extend the database of triggered creep from the EMC event by identifying and characterizing normal-faulting slip on many unrecognized structures within the central Imperial Valley. This slip occurred in regions where no field surveys were conducted after the 2010 earthquake. These faults are unmapped structures within the Brawley Seismic Zone that are about ~100 km from the El Mayor-Cucapah rupture. We determine the sense of motion and amount of slip, and we interpret their significance within the context of the San Andreas fault system and within the growing global dataset of coseismic slip observations.

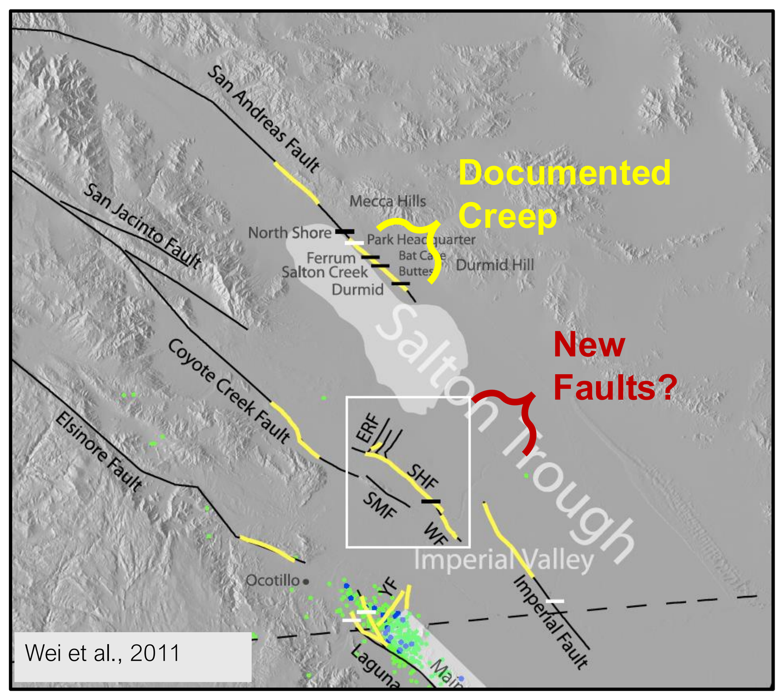

Dilatation Rate

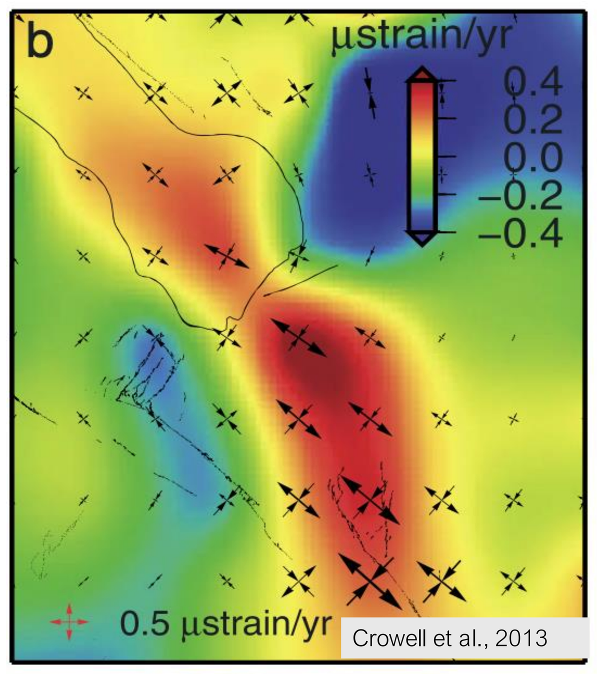

Remote Sensing Observations

- We find triggered slip that is evident in 16 coseismic UAVSAR interferograms and two coseismic EnviSAT interferograms, placing it tightly within the coseismic period. UAVSAR interferograms span 6-12 months and were collected one week after the earthquake. EnviSAT interferograms span 35 days between late March and mid May 2010. Together these interferograms bound the El Mayor Earthquake within a week on either side.
- The fractures are oriented slightly east of north and are concentrated on the south side of the Salton Sea Geothermal Field.
- The displacements are primarily vertical, as they have a similar sense of motion in both UAVSAR look directions.
- There are two polarities of displacements, as given by the phase increase or phase decrease across the fracture.
- We interpret these two polarities as representing two sides of a graben, one east-side-down and one west-side-down, rather than a single fault geometry that has both normal and reverse motion.
- In the bottom figure, East-side-down is shown in red; West-side-down is shown in blue.
- Recent observations made by UAVSAR in July 2025 show continued movement along one of these structures, which must be between 2018 and 2025.

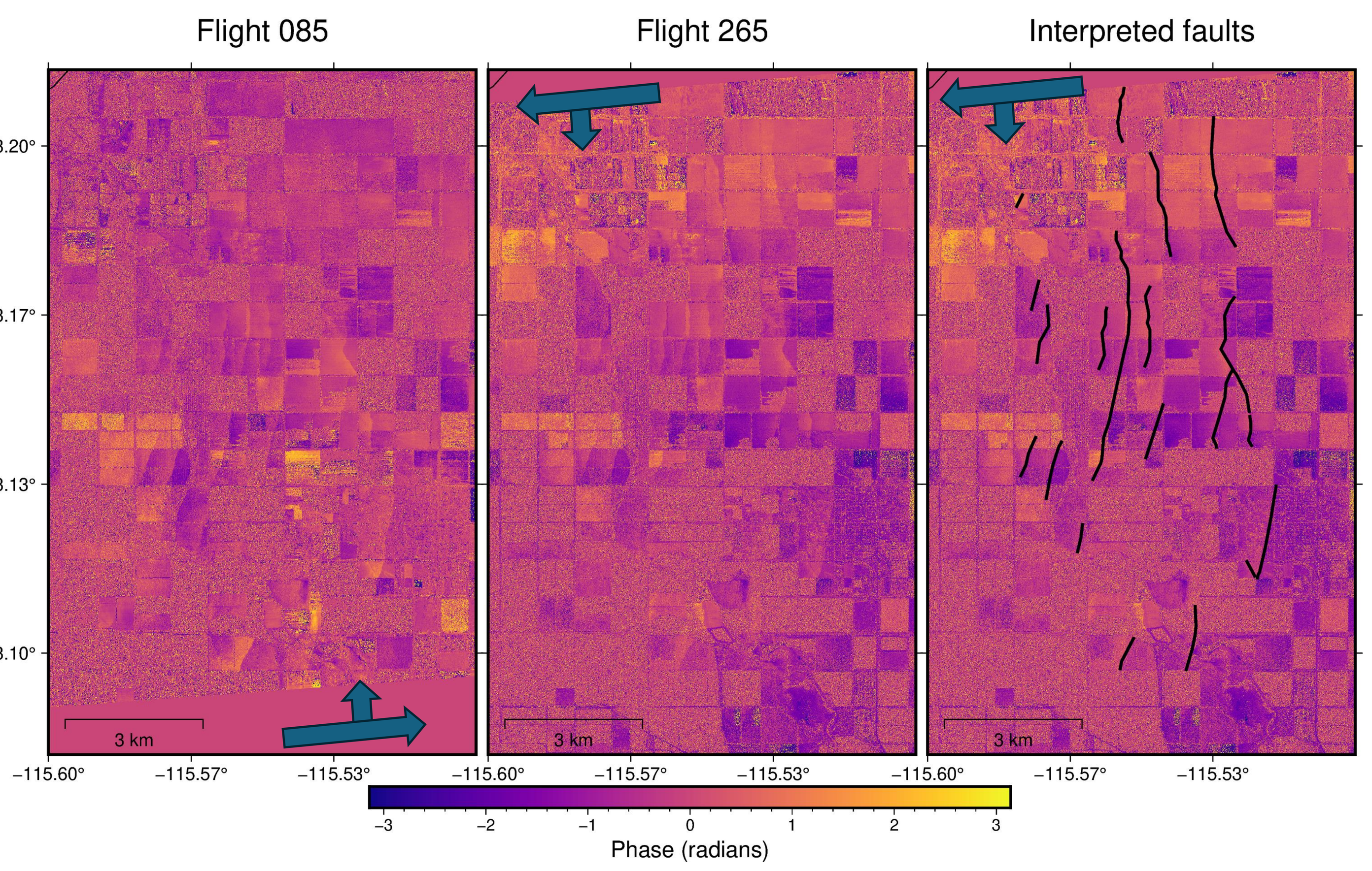

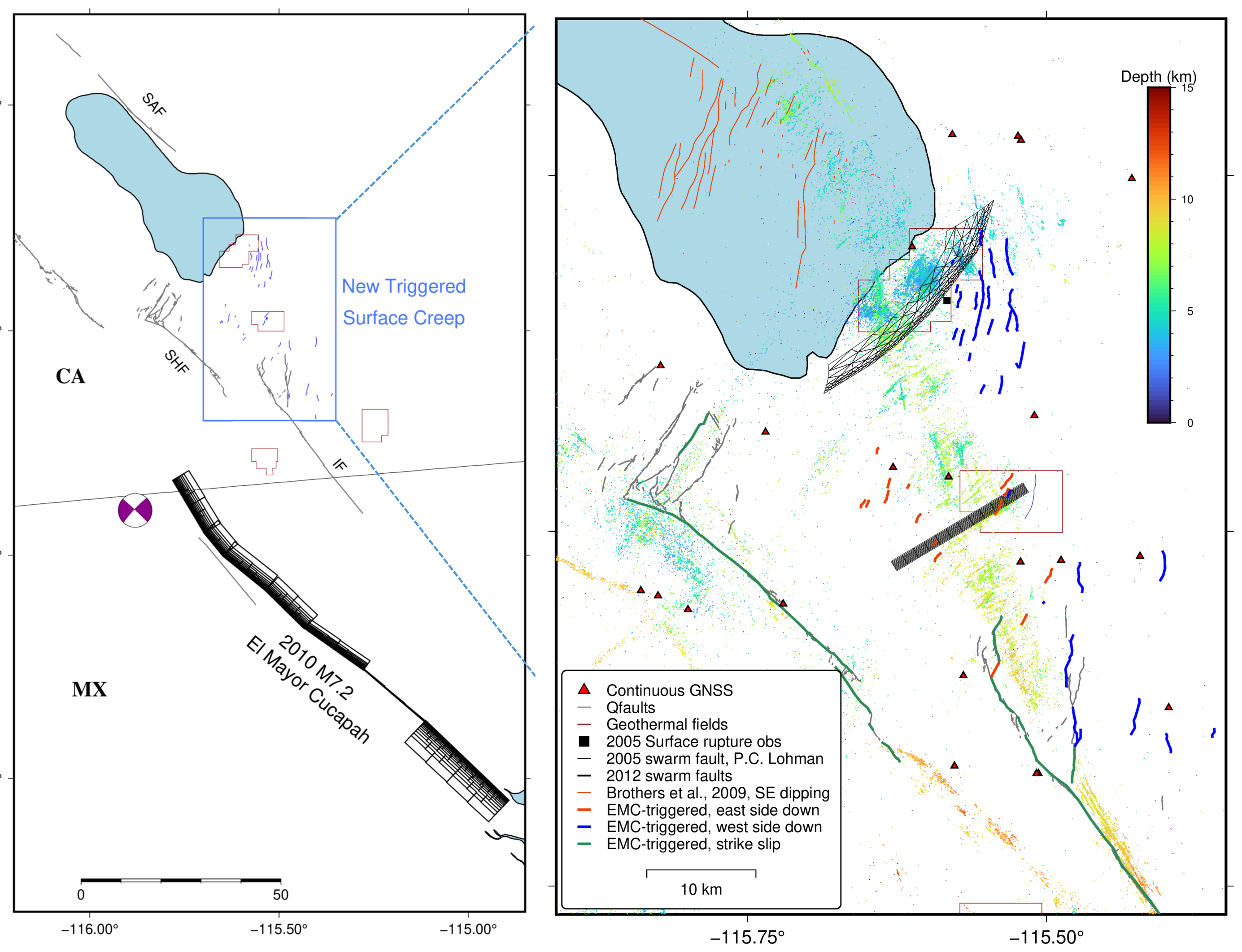

Displacement and Stress Modeling

We model displacements in the radar line-of-sight (LOS) using both UAVSAR flight directions (N85°E and N265°E). We use normal faults with a dip of 70° (based on Brothers et al., 2009). Pixels are masked based on coherence so that we ignore pixels with coherence < 0.3. The modeling calculates displacements in a homogeneous elastic half-space with a Poisson's ratio of 0.25 (Okada, 1992) and then projects them into each respective LOS. We track the look vector for every pixel because the incidence angle varies from 20—55° for UAVSAR.

The triggered slip amounts to 1-4 cm for each fracture that we have modeled thus far.

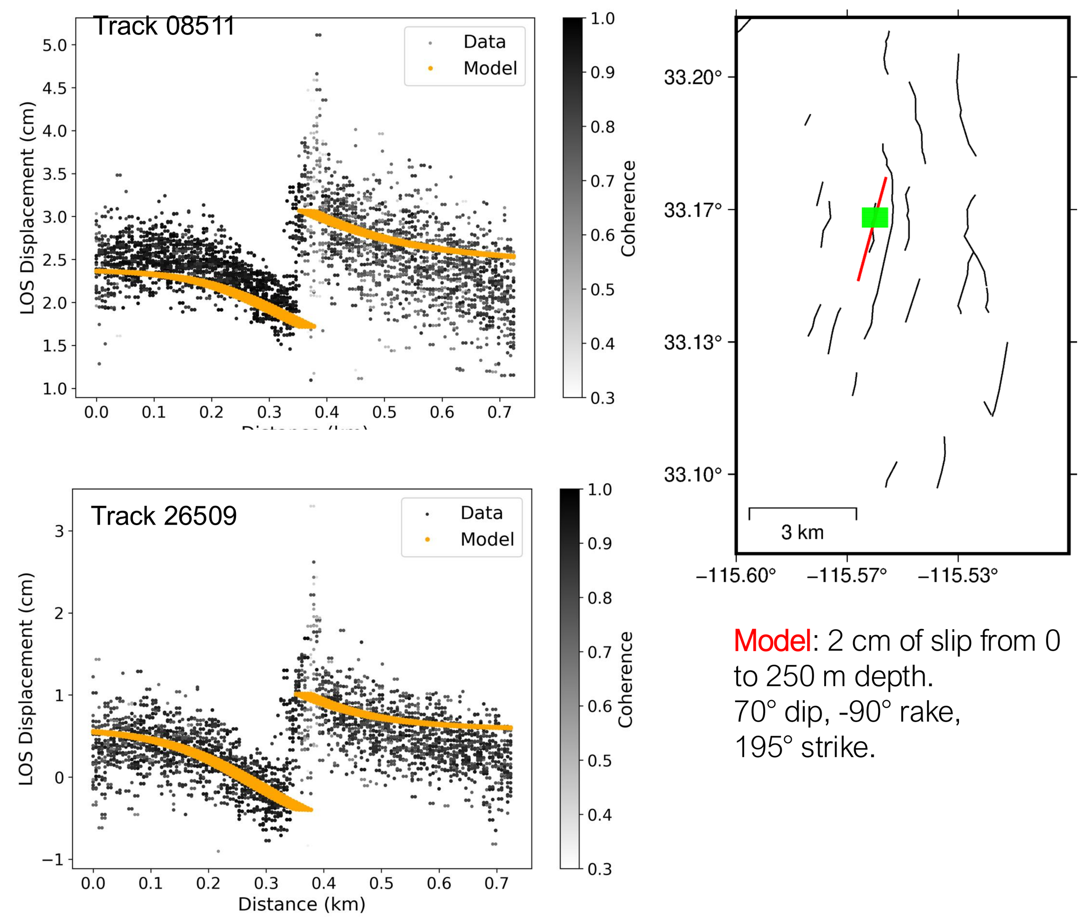

Model: 2 cm of slip from 0 to 250 m depth. 70° dip, -90° rake, 195° strike.

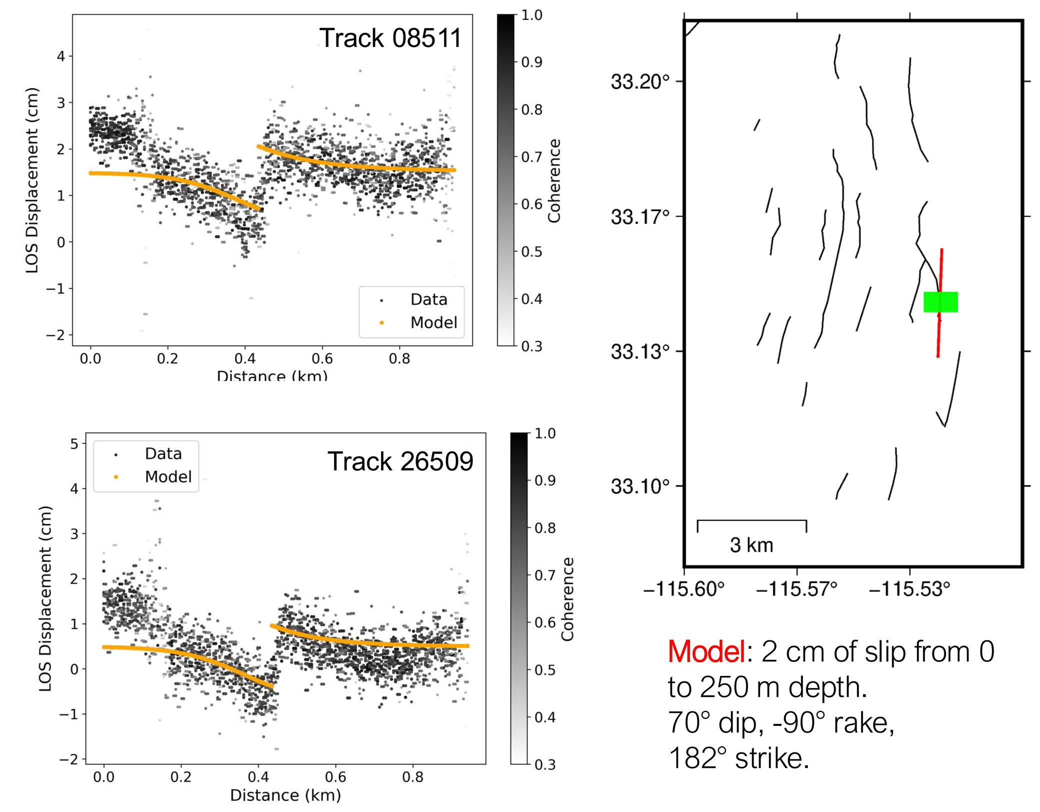

Model: 2 cm of slip from 0 to 250 m depth. 70° dip, -90° rake, 182° strike.

We computed the Coulomb Failure Stress applied to the newly recognized faults from the 2010 EMC earthquake. The peak CFS occurs when the rake is -90 (normal faulting) and is ~5 kPa of static stress increase. By contrast, the stress drop on these small fractures was potentially as high as 100 kPa.

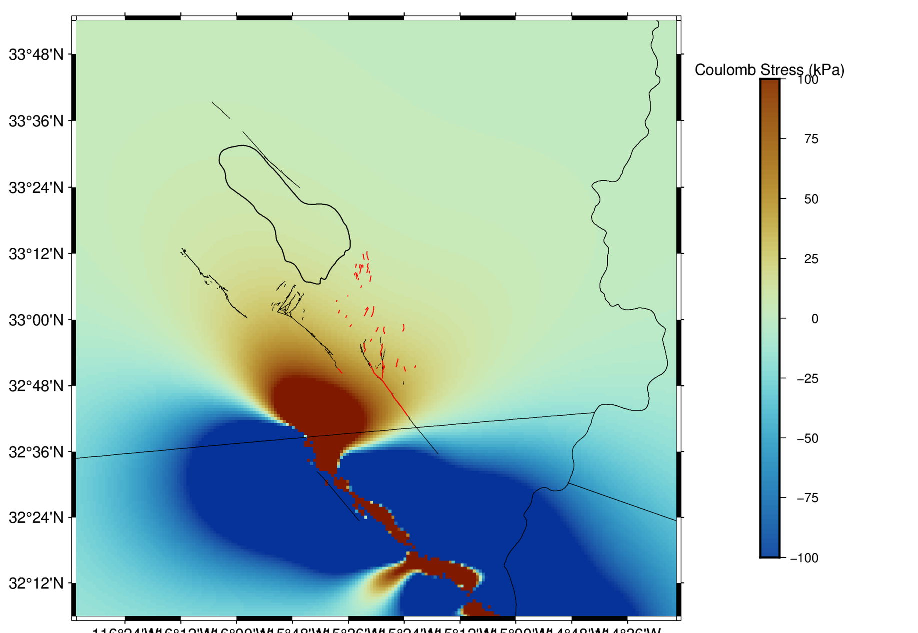

We have also noticed continued slip on newly-identified faults in UAVSAR interferograms from 2018-2025; the latest acquisition was collected in July 2025. This implies that these structures are long-lived, have ruptured multiple times, and continue to be active after the 2010 event. We are currently investigating a sequence of 12-day Sentinel-1interferograms to determine the more precise timing of the slip event.

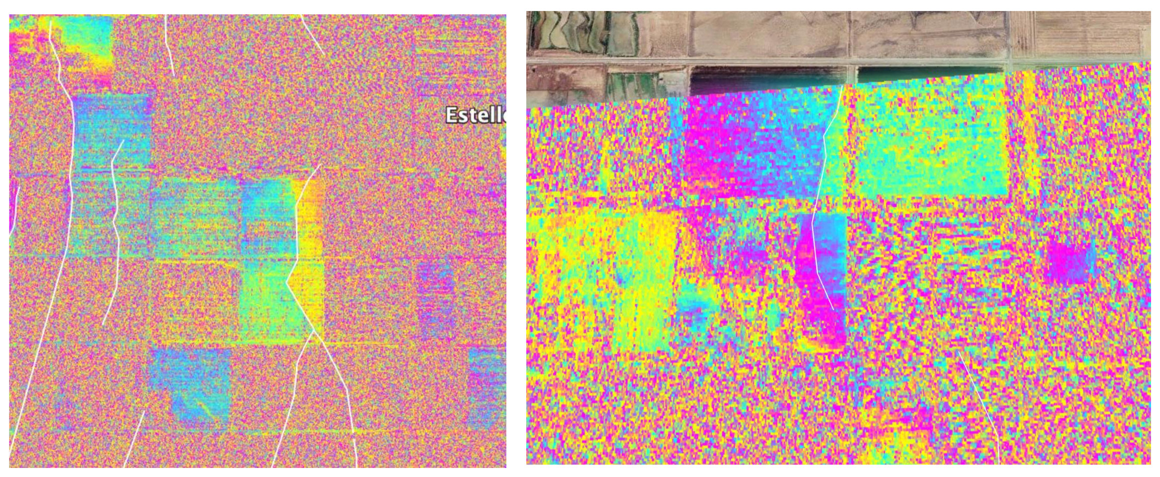

Tectonic Implications for the Salton Trough

These fractures likely accommodate extension and form shallow graben-like structure, consistent in orientation with the prevailing tectonic strain-rate direction (Elders et al, 1979; Crowell et al., 2013).
Based on their shapes, geometries, and sense of motion, these are the counterparts to the faults recognized in the seismic reflection survey of Brothers et al. (2009).
These faults may not be seismogenic sources themselves, but they are aseismically slipping. Still, they could be:

- Important pathways for fluid flow in geothermal areas.
- Play a role in accommodating extension and subsidence in the Salton Trough.
- Probe the material properties of the shallow subsurface such as rheology, frictional strength, and cohesion.

Further questions:

- Deeper seismicity is mostly left-lateral strike slip along bookshelf faults in the Brawley Seismic Zone. Does this imply a rotation of stress state with depth?
- The structure of the BSZ has been interpreted as an asymmetric basin (Brothers et al., 2009). Is the basin more symmetric than previously thought?
- How long-lived are these slipping structures? Do they release tectonic strain?
- What are the orientations of major structures in the geothermal area?

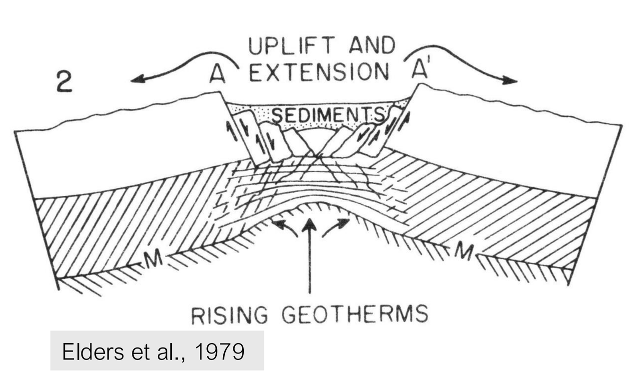

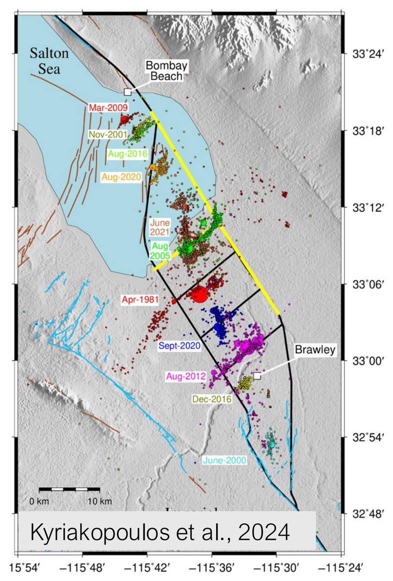

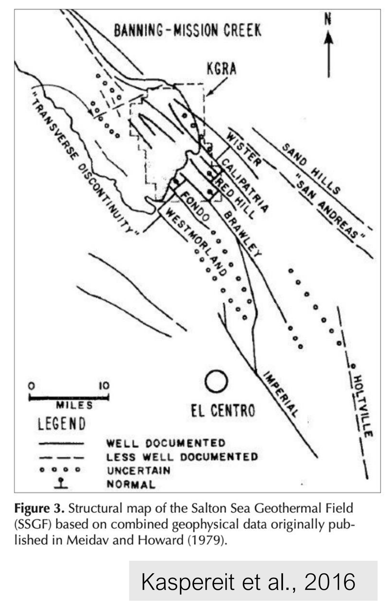

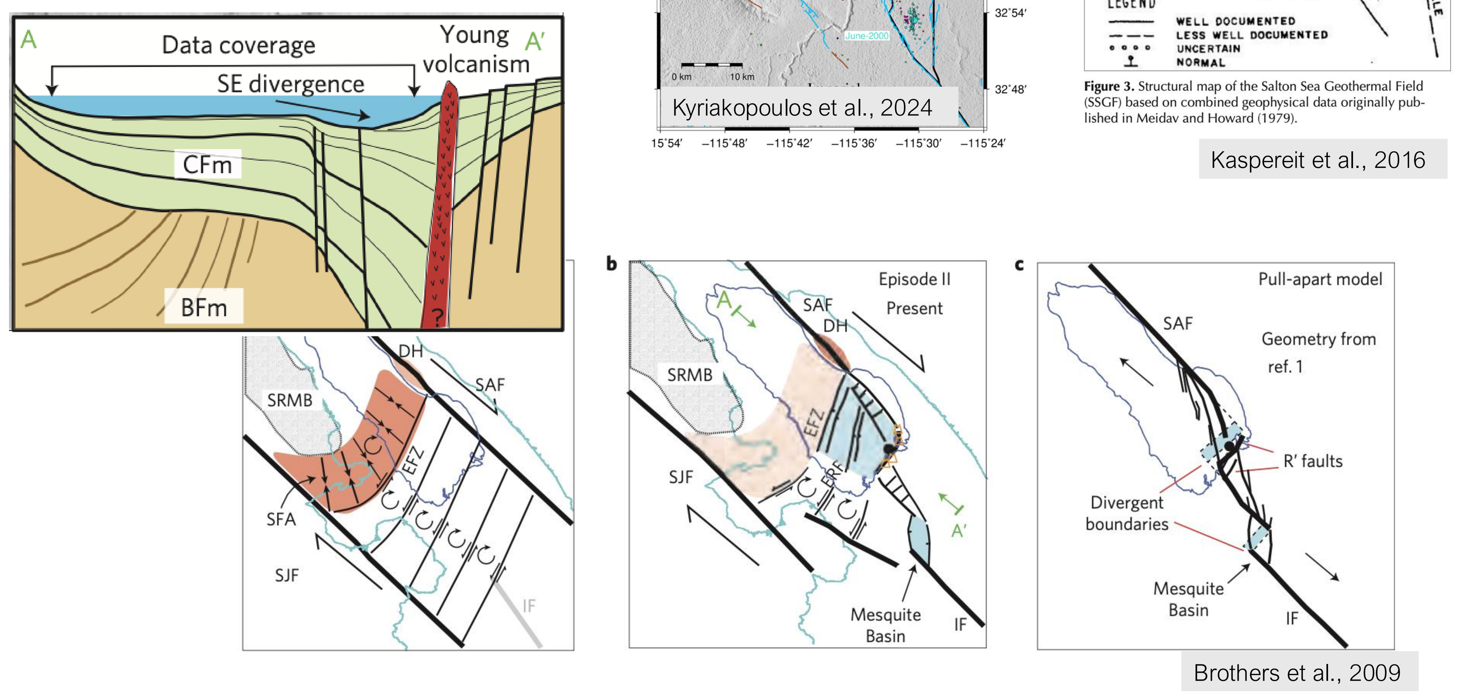

Triggered Slip Implications

Observations of earthquake-triggered slip and ground failure span a wide range of spatial scales and shaking intensities. Most recorded instances of triggered slip on small faults occur close to the main fault strand. A review by Valentini et al. (2025) classifies the effects of ground shaking into:

Seismo-tectonic:

- Primary fault slip
- Distributed faulting
- Secondary faulting (Sympathetic cracks)
- Triggered fault slip

Secondary:

- Lateral spreading due to gravitational forces
- Landslides
- Liquefaction
- Collapse of caves

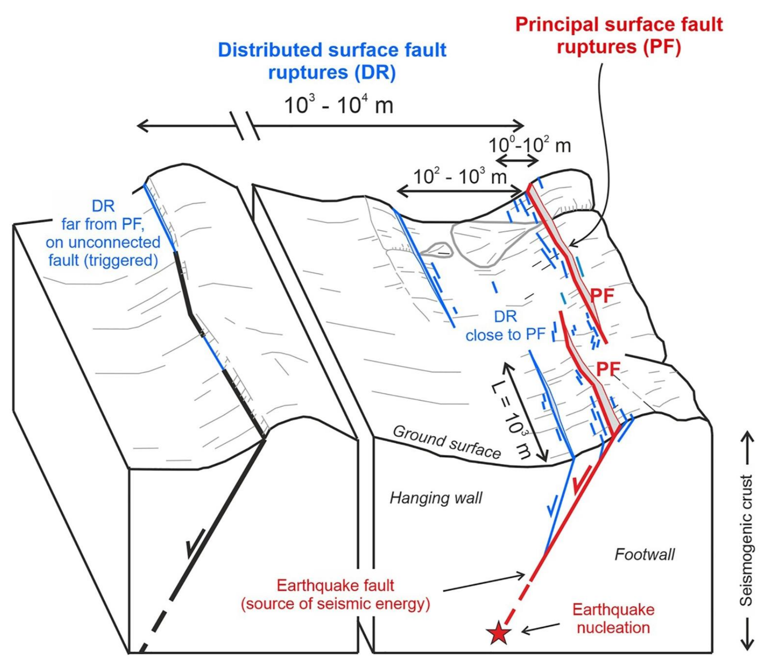

Valentini et al. (2025)

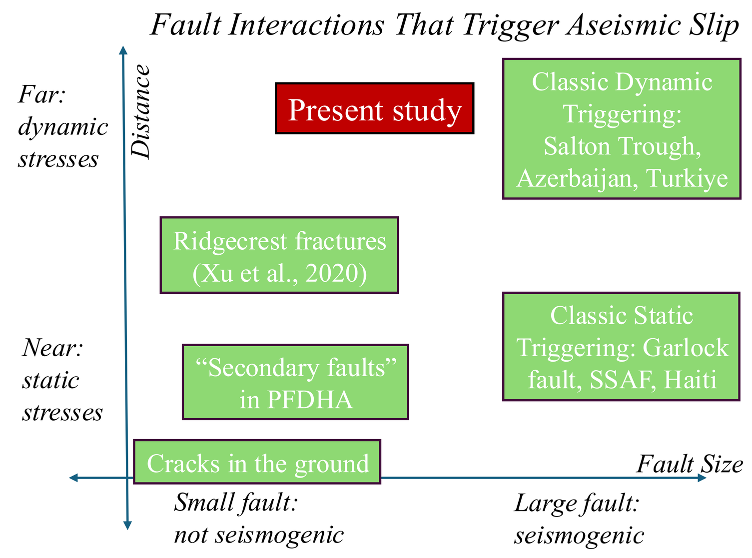

However, the current observations do not neatly fall into one of these categories. In this case, shaking at distances of ~50-100 km from the rupture, under PGA ~0.1g or MMI IV, produced ruptures of very small, previously unknown faults through dynamic shaking effects. This is closer to the observations of Xu et al. (2020) of the small-scale faults triggered to slip at medium distances by the 2019 Ridgecrest earthquake. These ruptures are not well understood.

Next Steps and Future Work

Dynamically triggered aseismic slip is commonly observed on large plate-bounding faults (e.g., Tymofyeyeva et al., 2019; Rymer et al., 2002). In the near-field of large ruptures, smaller secondary faults also commonly show triggered slip or surface displacement (Valentini et al., 2025). The current observations challenge the prevailing notion that large, plate-bounding faults may respond dynamic stresses in the far field, while smaller faults, cracks, and fractures respond to a range of stresses in the near field. The current observations are intermediate in distance and were likely triggered by dynamic stresses rather than static stresses, but the slip is not occurring on large, plate-bounding faults, which are often understood to be frictionally weak. The nearest analog so far is the triggered slip on medium-field faults in the Ridgecrest epicentral area (Xu et al., 2020). Displacement on secondary faults, in all their forms, have importance in the field of Probabilistic Fault Displacement Hazard Analysis (PFDHA), which determines the risk of damage to the built environment from fault slip. In the future, it is important to develop appropriate terminology and classification for a wide range of slip phenomena and identify analogous systems around the world as a first step to understanding the many modes of fault displacement.

References

Donnellan et al. (2014) https://doi.org/10.1002/2013GC005120; Wei et al. (2011) https://doi.org/10.1029/2010GL045235
Elders et al. (1979) "The geological background of the geothermal fields of the Salton Trough"
Wei et al. (2015) https://doi.org/10.1016/j.epsl.2015.06.044; Brothers et al. (2009) Nature Geoscience volume 2, pages 581–584
Crowell et al. (2013) https://doi.org/10.1002/jgrb.50347; Kyriakopoulos and Oglesby (2024) https://doi.org/10.1785/0220230326
Kaspereit et al. (2016) GRC Transactions, Vol. 40, 2016; Okada (1992) *Bulletin of the seismological society of America,* 82(2), 1018-1040.
Xu et al. (2020) DOI: 10.1126/science.abd1690; Valentini et al. (2025) https://doi.org/10.1029/2024RG000875
Rymer et al. (2002) https://doi.org/10.1785/0120000935; Rymer et al. (2011) https://doi.org/10.3133/ofr20101333.